Spectroscopic Investigation of Four Electronic States of NiF in the 17500−25000 cm^{-1} Region

Jin Jin, Qin Ran, Xueliang Yang, Yang Chen, and Congxiang Chen*

Open Laboratory of Bond-Selective Chemistry, and Department of Chemical Physics, University of Science and Technology of China, Hefei, 230026, China

Received: May 22, 2001; In Final Form: September 21, 2001

The laser-induced fluorescence excitation spectrum of jet-cooled NiF in the 17500−25000 cm^{-1} region has been recorded and analyzed, in which the NiF molecule was produced by the reaction of the sputtered nickel atoms with SF_6 under discharge conditions. Numerous bands are observed. With the help of the isotopic shift measurements and vibrational constants determined by B. Pinchemel's group, 26 bands have been vibrationally assigned. Twelve rotationally resolved transitions were found to originate from the ground state and terminate in different vibrational levels of four electronic states, [18.1] $^2\Delta_{5/2}$, [20.0] $^2\Delta_{5/2}$, [20.3] $\Omega = {}^3/_2$, and [22.9] $^2\Pi_i$, respectively. The molecular constants of these four upper states are determined. In addition, lifetime measurements of the four excited states were carried out under collision-free conditions. On the basis of the spectroscopic data and lifetime measurements, the electronic structure and interactions of these high-lying electronic states are discussed.

1. Introduction

Diatomic transition metal atom containing radicals, such as hydrides, oxides, and halides have received much attention during the past 50 years.[1−4] Gas-phase data of these species are helpful in understanding the complex role of the d electrons in bonding. Among the first-row transition metal halides, nickel monofluoride provides a simple model for the study of ionic bonding due to the strong electronegativity of the fluorine atom.

The complex electronic spectra of NiF have been studied in the visible spectral regions.[5−16] Many strong bands observed in this region have been rotationally analyzed or tentatively identified, and 10 electronic states were identified and summarized in an energy-level diagram[13] by Pinchemel's group. They predicted the molecular energy levels of electronic states of NiF on the basis of a ligand field model and compared it with the experimental observations.[17] As the weak $\Delta v \neq 0$ transitions in the emission spectra are often complex with complicated, overlapped band structure, most of the rotationally analyzed bands reported so far are 0−0 bands. In this work, the laser-induced fluorescence excitation spectrum of jet-cooled NiF in the 17500−25000 cm^{-1} region has been recorded and analyzed. With the help of the isotopic shift and vibrational constants determined by B. Pinchemel's group, 26 bands recorded in this region were vibrationally assigned. Most of the bands are $\Delta v \geq 0$ bands. Twelve bands involving different vibrational levels of four upper states, [18.1] $^2\Delta_{5/2}$, [20.0] $^2\Delta_{5/2}$, [20.3] $\Omega = {}^3/_2$, and [22.9] $^2\Pi_i$, and the ground-state $X^2\Pi_{3/2}$ have been rotationally analyzed. The molecular constants of these four high-lying excited states are determined for the first time. In addition, the lifetimes of the four excited states are measured under collision-free conditions, which gives evidence for the assignment of the electronic structures of these four electronic states.

* Corresponding author. E-mail: cxchen@ustc.edu.cn. Fax: +86-551-3607084.

2. Experiment

The DC discharge/reaction free jet expansion apparatus has been described in the earlier publications.[18,19] The NiF molecules were produced by the reaction of sputtered nickel atoms with SF_6/Ar mixture under discharge conditions. The sample gas, seeded in Ar at a stagnation pressure of 5 atm, passed through a pulsed nozzle (General Valve) of 0.5 mm orifice diameter at a repetition rate of 10 Hz into the vacuum chamber. The background pressures of the vacuum chamber were 3×10^{-2} and 2×10^{-3} Pa, respectively, with and without operation of the free jet.

The laser beam is the output of a tunable dye laser (Lumonics: HT-500) with a line width of 0.1 cm^{-1} and a pulse width of 5 ns pumped by a Nd: YAG laser (Spectra Physics: GCR-170) to excite the jet-cooled NiF molecules. The Nd: YAG laser and valve system were operated at 10 Hz. The dyes used were C540A, C500, C480, C460, C440, and EXA428 dye, which cover the 400−580 nm spectral region. The timing of the nozzle, discharge, and laser were controlled by a homemade pulse generator.

The laser-induced fluorescence from the excited NiF molecules was collected by means of a lens system, passed through a cutoff filter, and detected by a photomultiplier tube (GDB-56, Beijing). The signal was input to a computer for recording the spectrum, or to a transient digitizer (Tektronics TDS 380) for measuring the lifetime. For the calibration of the laser wavelength, we used optogalvanically active neon lines.

3. Results and Analysis

The excitation spectrum of jet-cooled NiF was recorded in the 17500−25000 cm^{-1} region. Numerous bands are observed, in which eight bands involving three high-lying $\Omega = {}^3/_2$ character states, [19.7] $^2\Pi_{3/2}$, [20.3] $\Omega = {}^3/_2$, and [22.9] $^2\Pi_{3/2}$, and two lower states, the ground-state $X^2\Pi_{3/2}$ and the low-lying state [0.25] $^2\Sigma$, have been rotationally analyzed in our recent paper,[19] and most of the transitions analyzed are 0−0 bands. In

10.1021/jp011972b CCC: $20.00
Published on Web 11/21/2001

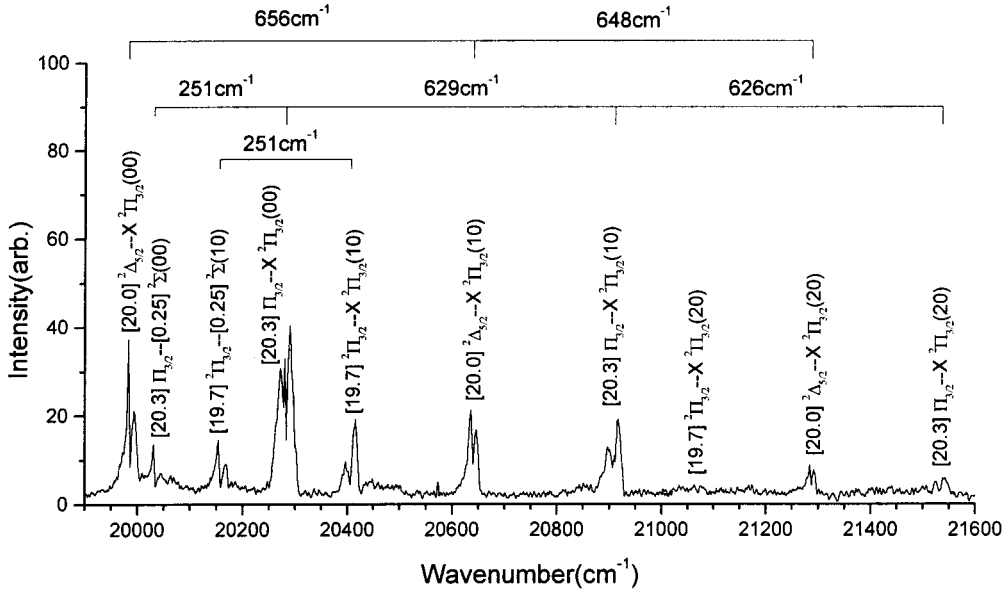

Figure 1. LIF excitation spectrum of NiF in the 19990−21600 cm^{-1} region.

this work, we rotationally analyze 12 electronic transitions involving different vibrational levels of four upper states, [18.1] $^2\Delta_{5/2}$, [20.0] $^2\Delta_{5/2}$, [20.3] $\Omega = {}^3/_2$, and [22.9] $^2\Pi_i$, and the ground-state $X^2\Pi_{3/2}$. Most of these are $\Delta v \geq 0$ bands, which makes it possible to obtain the complete molecular constants of these four high-lying electronic states, including vibrational constants ω_e and $\omega_e\chi_e$, rotational constants B_e and α_e, and internuclear distance R_e. In addition, the lifetimes of these four excited states are measured under collision-free conditions for the first time. This is of great help in assigning the electronic structures of the excited states of NiF.

3.1. Determination of the Symmetry of Upper Electronic States. It is well-known that the open d shell of transition metal atoms is generally responsible for the presence of low-lying states in corresponding diatomic molecules. NiF is one of the 3d-transition-metal atom containing species for which at least six low-lying electronic states have been observed in the first 2500 cm^{-1} above the ground state.[9−16] Both theoretical and experimental evidence exists which indicates that the $X^2\Pi_{3/2}$ state is the ground state with a very close-lying state $^2\Sigma$, 251 cm^{-1} above.[12−19] These two low-lying states are very close and can be populated simultaneously even at quite low temperature. As a result, the transitions with 251 cm^{-1} interval linking with these two low-lying states were observed in the laser-induced fluorescence spectrum[15,19] (see Figure 1). Because of the supersonic cooling associated with the experimental technique, only the ground state and the low-lying [0.25] $^2\Sigma$ state are populated. This allows us to determine the symmetry of the upper state easily.[19] According to the selection rule, $\Delta\Lambda = 0$, ± 1, and $\Delta S = 0$, the upper state may be $^2\Sigma$, $^2\Pi$, or $^2\Delta$, which will result in the transitions with different spectral features (for details see ref 19). For the bands which lack satellite transitions lying 251 cm^{-1} to the red, we can conclude that the symmetry of the upper state is $^2\Delta$. The two strong transitions at 18 108 and 19 983 cm^{-1} belong to such cases. They only link with the ground $X^2\Pi_{3/2}$ state. As a $^2\Delta$ state is always in Hund's case (a) coupling, the selection rule determines that the strong transitions recorded should be $^2\Delta_{5/2} \rightarrow X^2\Pi_{3/2}$ transitions. The presence of strong Q branches in their rotational structures confirms this assignment (see Figure 2). Therefore, the two upper states, [18.1] $^2\Delta_{5/2}$ and [20.0] $^2\Delta_{5/2}$, are identified, in which [18.1] $^2\Delta_{5/2}$ is consistent with the Pinchemel's result[14] and [20.0] $^2\Delta_{5/2}$ is reassigned. It had formerly been assigned as $^2\Pi_{1/2}$.[13] The

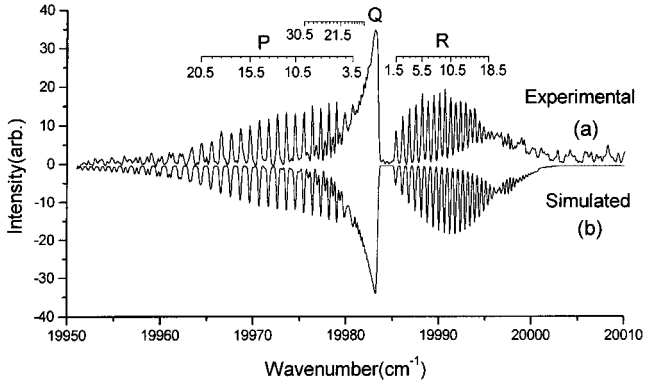

Figure 2. LIF spectrum of the 0−0 band of the [20.0] $^2\Delta_{5/2} \rightarrow X^2\Pi_{3/2}$ transition of NiF. (a) The upper trace is the experimental spectrum, and (b) the lower trace is the simulated spectrum.

identification of the three Π character states, [19.7] $^2\Pi_{3/2}$, [20.3] $\Omega = {}^3/_2$, and [22.9] $^2\Pi_i$ has been explained in detail in our previous paper.[19]

3.2. Vibrational Analysis and Isotopic Shift. Among the numerous bands recorded, there are six strong bands located at 18 107, 19 719, 19 983, 20 282, 22 955, and 23 498 cm^{-1}. On the basis of the intensities of the bands recorded (see Table 1), we tentatively assigned these six strong transitions as 0−0 bands. To the blue side of every strong 0−0 transition, there is at least one or more weak transitions with about 650 cm^{-1} interval, exhibiting similar spectral features (see Figure 1). As the vibrational constants of the high-lying electronic states determined by C. Focsa et al. are around 645 cm^{-1},[16] we attributed these weak transitions to 1−0, 2−0, and 3−0 bands relative to the strong transition. Also, the intensities of the 0−0, 1−0, 2−0, and 3−0 bands of one vibrational sequence are gradually decreasing, which is consistent with the vibrational analysis (see Table 1).

The vibrational assignment is further supported by the vibrational isotopic shifts observed in the weak $\Delta v \neq 0$ bands. It is well-known that nickel has two stable isotopes, ^{58}Ni and ^{60}Ni with a natural abundance ratio of about 2.6/1. Because of the rather large abundance of ^{60}Ni, the band lines and band heads of the isotopic molecule ^{60}NiF should appear with considerable intensity. As expected, the strong 0−0 band always shows a negligible isotopic shift in moderate resolution, while the weaker

TABLE 1: Assigned Vibrational Bands of NiF

transition (cm^{-1})	band (nm)	v−v	$\Delta\nu_{exp}$ (cm^{-1})	$\Delta\nu_{cal}$ (cm^{-1})	intensity
		[18.1] $^2\Delta_{5/2} \rightarrow X^2\Pi_{3/2}$			
18107.2	552.3	0−0	0	0.03(1)	30
18763.7	533.0	1−0	2.72(3)	2.71(3)	5
19415	515				1
		[20.0] $^2\Delta_{5/2} \rightarrow X^2\Pi_{3/2}$			
19983.5	500.4	0−0	0	0.02(1)	35
20639.0	484.5	1−0	2.71(3)	2.69(3)	17
21286.9	469.8	2−0	5.34(7)	5.36(4)	8
21927.0	456.0	3−0	8.1(2)	8.02(6)	3
		[19.7] $^2\Pi_{3/2} \rightarrow X^2\Pi_{3/2}$			
19719	507	0−0	0[a]	0.01(1)[a]	80
20406	490	1−0	1.93(4)[a]	2.65(4)[a]	15
21066	474.7	2−0	4.5(2)	5.30(5)	2
		[19.7] $^2\Pi_{3/2} \rightarrow$ [0.25] $^2\Sigma$			
19468	513.7	0−0	0		15
20155	496.0	1−0	1.9(1)		7
		[20.3] $\Omega = {}^3/_2 \rightarrow X^2\Pi_{3/2}$			
20282	493	0−0	0.86(6)[a]	0.02(2)[a]	35
20910	478	1−0	3.76(8)	2.67(4)	15
21536	464	2−0	6.5(1)	5.33(5)	5
		[20.3] $\Omega = {}^3/_2$−[0.25] $^2\Sigma$			
20031	499	0−0	0.9(1)		5
		[22.9] $^2\Pi_{3/2} \rightarrow X^2\Pi_{3/2}$			
22955	435.6	0−0	0	0.02(2)	90
23612	423.5	1−0	2.60(6)	2.69(3)	30
24260	412.1	2−0	5.37(9)	5.36(4)	10
		[22.9] $^2\Pi_{3/2} \rightarrow$ [0.25] $^2\Sigma$			
22703	440.5	0−0	0		40
23361	428.1	1−0			3
		[23.5] $^2\Pi_{1/2} \rightarrow X^2\Pi_{3/2}$			
23498	425.5	0−0	0	0.01(2)	60
24149	414.0	1−0	2.6(1)	2.66(8)	12
24793	403.3	2−0	5.0(2)	5.31(9)	2
		[23.5] $^2\Pi_{1/2} \rightarrow$ [0.25] $^2\Sigma$			
23247	430.1	0−0			7
23898	418.4	1−0			1

[a] From ref 19; $\Delta\nu_{cal}$ refers to the ^{58}NiF−^{60}NiF isotopic shift calculated by eq 1 (see text).

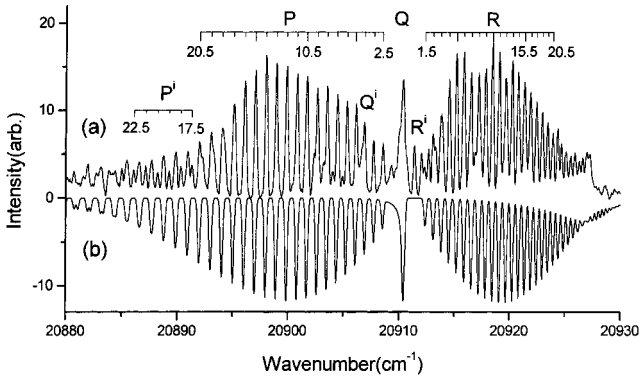

Figure 3. LIF spectrum of the 1−0 band of the [20.3] $\Omega = {}^3/_2 \rightarrow X^2\Pi_{3/2}$ transition of NiF. (a) The experimental spectrum, rotational lines belonging to isotopomer ^{60}NiF are easily recognized in P^i, Q^i, and R^i branches. (b) The simulated spectrum for ^{58}NiF.

1−0, 2−0, and 3−0 bands present observable and gradually increasing isotopic shifts (see Figures 3 and 4). The measured isotopic shifts between the Q heads of ^{58}NiF and ^{60}NiF are listed in Table 1. To the first order, the isotopic shifts can be derived by the following equation:[20]

$$\Delta\nu = \nu - \nu^i = (1-\rho)\,[\omega_e(v+1/2) - \omega_e(v+1/2)] \quad (1)$$

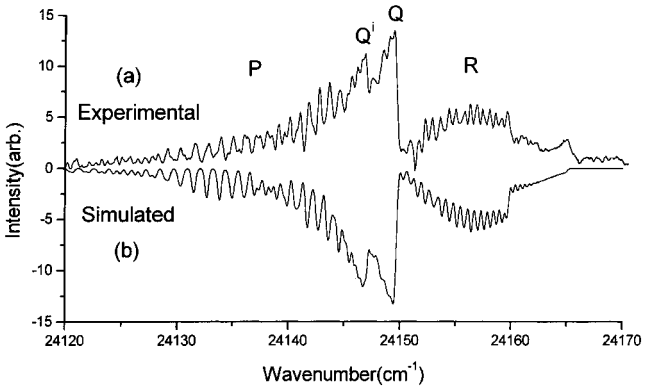

Figure 4. LIF spectrum of the 1−0 band of the [23.5] $^2\Pi_{1/2} \rightarrow X^2\Pi_{3/2}$ transition of NiF. (a) The experimental spectrum; Q^i is the Q head belonging to isotopomer ^{60}NiF. (b) The simulated spectra for the ^{58}NiF and ^{60}NiF isotopomers.

where $\rho = [\mu(^{58}\text{NiF})/\mu(^{60}\text{NiF})]^{1/2} \approx 0.99588$. The vibrational isotopic shifts due to the two main Ni isotopes are calculated using the vibrational constants in the Table 1 of ref 13 and listed in Table 1 of this work. In the calculation, we used an average value 645 cm^{-1} for the newly reported [20.3] $\Omega = {}^3/_2$ state. We noticed that most of the measured isotopic shifts are consistent with the calculated ones, but some discrepancies exist in the transitions with upper state [19.7] $^2\Pi_{3/2}$ and [20.3] $\Omega = {}^3/_2$, which will be discussed in section 4.3.

3.3. Rotational Analysis and Simulation. From the above analysis, the six bands located at 18 107, 18 763, 19 983, 20 639, 21 287, and 21 927 cm^{-1} are assigned as $^2\Delta_{5/2} \rightarrow X^2\Pi_{3/2}$ transitions. They all exhibit regular P and R branches and a strong Q branch (see Figure 2a). The rotational analysis shows that the first R lines of all transitions correspond to $J'' = {}^3/_2$, implying that the lower state of these transitions has $\Omega = {}^3/_2$. This is consistent with the fact that the lower state is the ground $X^2\Pi_{3/2}$ state. The presence of a strong Q branch and the first P lines corresponding to $J'' = {}^7/_2$ indicates that these transitions are $^2\Delta_{5/2} \rightarrow X^2\Pi_{3/2}$ transitions. Fine structure is observed in the P branch of the strong 0−0 band of $^2\Delta_{5/2} \rightarrow X^2\Pi_{3/2}$ transition (see Figure 2a). The splittings increase proportionally to J^3 when $J \geqslant 22.5$ in the two intense 18 107 and 19 983 cm^{-1} bands. This is due to lambda doubling in the $X^2\Pi_{3/2}$ state. Splittings of the lines in the weaker $\Delta v \neq 0$ bands are not observed clearly, due to the weaker intensities of these futures and the isotope shift.

Four weaker bands at 20 910, 21 536, 23 612, and 24 260 cm^{-1} are assigned as $^2\Pi_{3/2} \rightarrow X^2\Pi_{3/2}$ transition. They exhibit strong P and R branches and a weak blended Q branch. As $\Delta v \neq 0$ bands, rotational lines belonging to the ^{60}NiF isotopomer are easily recognized in some lines of P, Q, and R branches (see Figure 3a). The first observed lines of the R and P branches are R(1.5) and P(2.5), respectively, indicating an $\Omega = {}^3/_2 \rightarrow \Omega = {}^3/_2$ transition. All these spectroscopic characteristics are consistent with those of a $^2\Pi_{3/2} \rightarrow X^2\Pi_{3/2}$ transition. It is possible that the upper [20.3] $\Omega = {}^3/_2$ state is a $^2\Delta_{3/2}$ state or primarily quartet in character, as is discussed more fully in section 4.2. The two bands at 23 498 and 24 149 cm^{-1} are assigned as $^2\Pi_{1/2} \rightarrow X^2\Pi_{3/2}$ transitions. Both of them show P and R branches and a strong Q branch, exhibiting fine structure. Two parameters are necessary to account for this fine structure. The presence of a linear with J parameter suggests that the projection Ω of the total angular momentum on the internuclear axis is equal to $^1/_2$. The second parameter increased with J^3, caused by the lambda doubling in the $X^2\Pi_{3/2}$ state. In addition, the transition lying 251 cm^{-1} to the red of 23 498 cm^{-1} transition

TABLE 2: Rotational Constants (in cm^{-1}) for the Twelve Transitions of NiF[a]

state	v	T_v	B_v	D_v ($\times 10^{-6}$)	a ($\times 10^{-4}$)/p
[23.5] $^2\Pi_{1/2}$	0	23498.50(8)	0.3793(1)	0.47(5)	−0.154(4)
		23498.60(2)[b]	0.37922(3)[b]	0.47(2)[b]	−0.152(2)[b]
	1	24149.50(8)	0.3761(2)	0.47(6)	−0.135(6)
	1[i]	24147.20(9)	0.3730(2)	−	−
[22.9] $^2\Pi_{3/2}$	0	22955.05(8)[c]	0.3794(1)[c]	0.47(3)[c]	0[c]
		22955.12(2)[b]	0.37928(3)[d]	0.469(3)[d]	
	1	23611.80(8)	0.3760(2)	0.47(3)	0
	1[i]	23609.20(9)	0.3729(3)	−	−
	2	24260.22(9)	0.3729(2)	0.46(5)	0
	2[i]	24254.85(9)	0.3700(3)	−	−
[20.3] $\Omega = {}^3/_2$	0	20281.96(7)[c]	0.3844(1)[c]	0.65(5)[c]	−0.06(2)[c]
	0[i]	20281.10(2)[c]	0.3807(4)[c]	0.64(8)[c]	−
	1	20910.46(2)	0.3811(2)	0.60(5)	−0.05(2)
	1[i]	20906.7(1)	0.3777(3)	−	−
	2	21536.32(2)	0.3778(2)	0.60(5)	0
	2[i]	21529.76(2)	0.3746(4)	−	−
[20.0] $^2\Delta_{5/2}$	0	19983.46(2)	0.3795(1)	0.45(1)	
		19983.453(6)[d]	0.379484(2)[d]	0.446(1)[d]	
	1	20639.08(2)	0.3764(1)	0.45(2)	
	1[i]	20636.37(2)	0.3732(2)	−	
	2	21286.90(2)	0.3734(2)	0.40(5)	
	2[i]	21281.56(2)	0.3700(3)	−	
	3	21927.45(5)	0.3702(2)	0.4(1)	
[18.1] $^2\Delta_{5/2}$	0	18107.25(2)	0.3790(1)	0.46(2)	
		18107.55(1)[d]	0.379058(3)[d]	0.459(1)[d]	
	1	18763.72(2)	0.3760(1)	0.45(2)	
	1[i]	18761.00(3)	0.3728(2)	−	
$X^2\Pi_{3/2}$	0	0	0.3877(1)	0.55(3)	−0.10(1)
		0	0.38774(4)[d]	0.551(2)[d]	−0.1045(1)[d]
	0[i]	0	0.3845(2)	0.54(5)	−

[a] "i" refers to isotopomer ^{60}NiF. [a] From ref 15. [b] From ref 19. [c] From ref 14.

shows a typical pattern of a $^2\Pi_{1/2} \rightarrow {}^2\Sigma$ transition. So we think the experimental $\Omega = {}^1/_2$ state (23498 cm^{-1}) may be the theoretically calculated $^2\Pi_{1/2}$ (23504 cm^{-1}).[17] As the ground state is a pure Hund's case (a) $^2\Pi_{3/2}$ state, the transition occurs because the upper [23.5] $^2\Pi_{1/2}$ state is mixed via spin−orbit interaction with a $^2\Sigma$ state. The identification of the [23.5] $^2\Pi_{1/2}$ state is consistent with the Pinchemel's result.[14,15] Figure 4a presents the LIF spectrum of the 1−0 band of the [23.5] $^2\Pi_{1/2} \rightarrow X^2\Pi_{3/2}$ transition of NiF, in which the Q head belonging to the ^{60}NiF isotopomer is readily recognizable.

Rotational simulations were carried out to determine the spectroscopic constants of the upper and lower states of each transition. We use the following expression [2] [22] for the upper $^2\Delta_{5/2}$, the expression [3] [20] for the upper $^2\Pi_{3/2}$ and $^4\Pi_{3/2}$ states, and the expression [4] [20] for the upper $^2\Pi_{1/2}$ in Hund's case (a) coupling

$$T_{e\,or\,f} = T_v + B_v J(J+1) - D_v J^2(J+1)^2 \qquad (2)$$

$$T_{e\,or\,f} = T_v + B_v J(J+1) - D_v J^2(J+1)^2 \pm a(J-1/2)(J+1/2)(J+3/2) \qquad (3)$$

$$T_{e\,or\,f} = T_v + B_v J(J+1) - D_v J^2(J+1)^2 \pm 1/2p(J+1/2) \qquad (4)$$

where the plus and minus signs refer to the e and f rotational levels, respectively. And expression 3 is also used for the ground-state $X^2\Pi_{3/2}$ which is near Hund's case (a) coupling. In the simulation, the line shape was convoluted with a Lorentzian function and the intensities of the rotational lines in each band were given by the combination of the Hönl-London factor[20,21] and the Boltzmann distribution (T_{rot} about 95 K). Expressions 2 and 3, and the Hönl−London factors for $\Delta\Lambda = 1$, $\triangle\Omega = 1$ transition were used for the $^2\Delta_{5/2} \rightarrow X^2\Pi_{3/2}$ transition. Expression 3 and the Hönl−London factors for the $\Delta\Lambda = 0$, $\triangle\Omega = 0$ transition were used for the $^2\Pi_{3/2} \rightarrow X^2\Pi_{3/2}$ transition. The simulated spectra of these transitions are shown in Figure 2b and Figure 3 b, which are in good agreement with the experimental ones. Expressions 4 and 3 and the Hönl−London factors for the $\Delta\Lambda = 0$, $\triangle\Omega = -1$ transition were used for the $^2\Pi_{1/2} \rightarrow X^2\Pi_{3/2}$ transition (see Figure 4b). The rotational constants derived from the simulation are summarized in Table 2. In addition, in the weak $\Delta v \neq 0$ bands, some rotational lines corresponding to the second ^{60}Ni isotope appear, whose intensities are in agreement with the natural abundance. The rotational constants of the isotopic species ^{60}NiF obtained from the simulations are listed in Table 2, which are in good agreement with the values calculated individually by the equation: $B^i = \rho^2 B$, where $\rho = [\mu(^{58}\text{NiF})/\mu(^{60}\text{NiF})]^{1/2} \approx 0.99588$.

Now, 12 bands involving different vibrational levels of four upper states, [18.1] $^2\Delta_{5/2}$, [20.0] $^2\Delta_{5/2}$, [20.3] $\Omega = {}^3/_2$, and [22.9] $^2\Pi_i$, and the ground-state $X^2\Pi_{3/2}$ have been rotationally analyzed and their rotational constants are derived. The line positions of the transitions are collected in Table 5S. As the most bands analyzed are $\Delta v \geq 0$ bands, combined with the previous results of the 0−0 bands,[19] the molecular constants of these four high-lying excited states including vibrational constants ω_e and $\omega_e\chi_e$, rotational constants B_e and α_e, and internuclear distance R_e are determined for the first time and listed in Table 3.

3.4. Lifetime Measurement. The lifetimes of different vibrational levels of the five upper states, [18.1] $^2\Delta_{5/2}$, [19.7] $^2\Pi_{3/2}$, [20.0] $^2\Delta_{5/2}$, [20.3] $\Omega = {}^3/_2$, and [22.9] $^2\Pi_i$, were measured by using a pulsed dye laser excitation. For each sub-band, we selected one rotational level. To avoid fluctuations and improve the signal-to-noise ratio, the fluorescence decay profiles were averaged over 256 laser shots. As the NiF radical is present in the supersonic jet, the excited state lifetime measurement may

TABLE 3: Molecular Constants (in cm^{-1}) for the Four Excited States of NiF[a]

state	T_e	ω_e	$\omega_e\chi_e$	B_e	α_e	R_e (Å)
[23.5] $^2\Pi_{1/2}$	23498.5	658.50	3.75	0.3807	3.1	1.759
	23498.60[b]	643.28[c]				
[23.5] $^2\Pi_{1/2}$[i]	23498.5	656.30	3.80			
[22.9] $^2\Pi_{3/2}$	22955.06	665.06	4.16	0.3809	3.25	1.758
	22955.12[b]	648.23[c]				
[22.9] $^2\Pi_{3/2}$i	22955.1	662.63	4.25	0.3773	2.9	1.758
[20.3] $\Omega = {}^3/_2$	20281.96	631.14	1.32	0.3860	3.3	1.747
[20.3] $\Omega = {}^3/_2$[i]	20281.08	628.18	1.28	0.3823	3.05	1.748
[20.0] $^2\Delta_{5/2}$	19983.46	663.35	3.88	0.3810	3.1	1.758
	19983.453[d]	647.55[c]				
[20.0] $^2\Delta_{5/2}$[i]	19983.5	660.63	3.86	0.3780	3.2	1.758
[18.1] $^2\Delta_{5/2}$	18107.25	661.62	2.58	0.3805	3.0	1.759
	18107.55[d]	651.37[c]	0.66[c]			

[a] "i" refers to isotopomer ^{60}NiF. [b] From ref 15. [c] From ref 16. [d] From ref 14.

TABLE 4: Lifetime (in μs) of the Different Vibrational Levels of the Five Excited States in NiF

state	T_o (cm^{-1})	$v' = 0$	$v' = 1$	$v' = 2$	$v' = 3$
[23.5] $^2\Pi_{1/2}$	23498.5	0.45(2)	0.46(2)		
[22.9] $^2\Pi_{3/2}$	22955.0	0.36(2)	0.38(2)	0.41(2)	
[20.3] $\Omega = {}^3/_2$	20281.96	1.8(1)	1.8(1)	1.9(1)	
[19.7] $^2\Pi_{3/2}$	19719.0	1.6(1)	1.5(1)	1.6(1)	
[20.0] $^2\Delta_{5/2}$	19983.5	1.7(1)	1.3(1)	1.4(1)	1.2(2)
[18.1] $^2\Delta_{5/2}$	18107.25	3.3(1)	3.4(1)		

be considered as occurring under collision-free conditions. Therefore, the radiative lifetime of the excited state can be directly derived from the decay of the fluorescence signal. Figure 5 illustrates a typical fluorescence decay curve obtained following excitation of the 0−0 band of the [22.9] $^2\Pi_{3/2} \rightarrow X^2\Pi_{3/2}$ transition. The lifetime of the upper state of each band could be easily derived by fitting the signal to a monoexponential decay and are listed in Table 4. The lifetimes of different excited electronic states are noticeably different. The [22.9] $^2\Pi_i$ state of NiF has the shortest lifetime, only about 0.4 μs, while the [18.1] $^2\Delta_{5/2}$ state has the longest, around 3μs. The remaining three states, [19.7] $^2\Pi_{3/2}$, [20.0] $^2\Delta_{5/2}$, and [20.3]$\Omega = {}^3/_2$, have similar lifetimes, near 1.6 μs.

4. Discussion

4.1. Excited States, Lifetimes, and Electronic Structure. On the basis of the spectroscopic data, the reported theoretical calculations,[17] and lifetime measurements, we may conjecture the electronic structure of the five excited states, [18.1] $^2\Delta_{5/2}$, [19.7] $^2\Pi_{3/2}$, [20.0] $^2\Delta_{5/2}$, [20.3]Ω = 3/2, and [22.9] $^2\Pi_i$. All these five excited electronic states correspond to electron configurations of $3d^8(^1D)4s^1$ on the Ni^+ ion. Compared to the theoretical result,[17] the [22.9] $^2\Pi_i$ state with the shortest lifetimes in the range of 0.35−0.5 μs could derive from the $3d^8(^3P)4s^1$, ^2P atomic ion limit. Three excited states with similar lifetimes (1.2−1.9 μs), [19.7] $^2\Pi_{3/2}$, [20.0] $^2\Delta_{5/2}$, and [20.3] Ω = 3/2, all derive from the $3d^8(^1D)4s^1$, ^2D atomic ion limit. The remaining [18.1] $^2\Delta_{5/2}$ states having the longest lifetime (3.3−3.4μs) may derive from the $3d^8(^3F)4s^1$, ^2F Ni^+ ionic limit. If the above assignment is true, we may conclude that the states with different excited-state lifetimes correlate with different Ni^+ ionic limits while the states with similar excited-state lifetimes all derive from the same Ni^+ atomic term.

4.2. Possible Candidates of [20.3] $\Omega = {}^3/_2$ State. From the former analysis,[19] the 20 282 cm^{-1} transition has been assigned as the [20.3] $\Omega = 3/2 \rightarrow X^2\Pi_{3/2}$ transition, and the upper state is well characterized by $\Omega' = 3/2$ and may correlate to the $3d^8(^1D)4s^1$, ^2D atomic ion limit. Theoretical calculations show that there are only two $\Omega = {}^3/_2$ states, one $^2\Pi_{3/2}$ and one $^2\Delta_{3/2}$, in the 17000−22000 cm^{-1} energy region, associated with ^2D ionic limit.[17] The experimental [19.7] $^2\Pi_{3/2}$ state has already been identified as the theoretically calculated $^2\Pi_{3/2}$ (19120 cm^{-1}) state,[14,17,18] so the newly identified [20.3] $\Omega = {}^3/_2$ state may be a $^2\Delta_{3/2}$ state. In addition, the intensity of the 0−0 band of [20.3]$\Omega = {}^3/_2 \rightarrow X^2\Pi_{3/2}$ transition is less than a half of that of the [19.7] $^2\Pi_{3/2} \rightarrow X^2\Pi_{3/2}$ 0−0 band. This also indicates that the upper state may be a $^2\Delta_{3/2}$ state. The oscillator strength that makes a forbidden $^2\Delta_{3/2} \rightarrow X^2\Pi_{3/2}$ transition derives from an admixture of $^2\Pi_{3/2}$ character in the upper state.[23] In this case, it is the nearby [19.7] $^2\Pi_{3/2}$ state which is undoubtedly mixed with the [20.3] $\Omega = {}^3/_2$ state. If we consider that the true molecular states of NiF molecules are arising from a set of Hund's case a basis states that are coupled via the spin−orbit interaction, then the possible candidates which can mix with the $^2\Pi_{3/2}$ state that provides the source of the oscillator strength for this transition could be $^2\Delta_{3/2}$, $^4\Sigma_{3/2}$, $^4\Pi_{3/2}$, and $^4\Delta_{3/2}$ according to the following selection rules: $\Delta S = 0, \pm1$; $\Delta\Lambda = 0, \pm1$; $\Delta\Sigma = 0, 1$.[23] Of these possibilities, it is more likely that this [20.3] $\Omega = {}^3/_2$ state could be the $\Omega = {}^3/_2$ component of the [20.0] $^2\Delta_{5/2}$ state, since this $^2\Delta_{3/2}$ state would fluoresce to the $^2\Pi_{1/2}$ component of the ground state with a fluorescence rate similar to that of the [20.0] $^2\Delta_{5/2}$ state to the $X^2\Pi_{3/2}$ component of the ground state. On the other hand, the [20.3] $\Omega = {}^3/_2$ state is unusual, having molecular constants and internuclear distances that are significantly different from those of doublet electronic states nearby (see Table 3). Because of this, we think it is possible that the upper [20.3] $\Omega = {}^3/_2$ state is primarily quartet in character, since the theoretical calculations[17] show that there is a $^4\Pi_{3/2}$ state (19030 cm^{-1}) near a $^2\Pi_{3/2}$ state in the 17000−22000 cm^{-1} energy region.

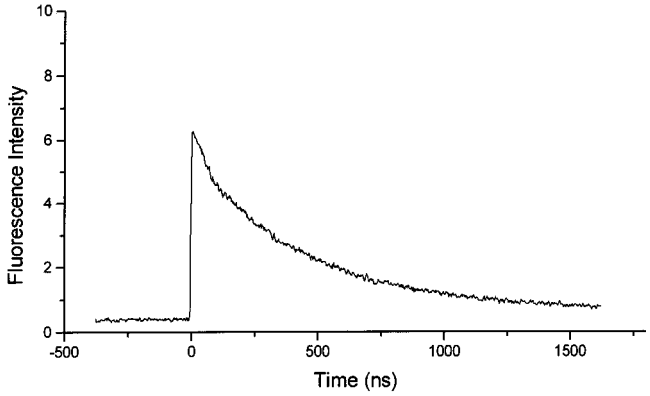

Figure 5. Typical fluorescence decay curve, recorded following excitation of the 0−0 band of the [22.9] $^2\Pi_{3/2} \rightarrow X^2\Pi_{3/2}$ transition of NiF.

4.3. Interaction between [19.7] $^2\Pi_{3/2}$ and [20.3] $\Omega = {}^3/_2$ Sstates. From Table 1, it can be seen that the measured isotopic shifts in the $v = 1$ and $v = 2$ levels of the [19.7] $^2\Pi_{3/2}$ state, and the $v' = 0$, 1, and 2 levels of the [20.3] $\Omega = {}^3/_2$ state are significantly different from the calculated ones. In addition, the $\Delta G_{1/2}$ value of the [19.7] $^2\Pi_{3/2}$ state is unusually large, about 688 cm^{-1}, compared to other high-lying electronic states of NiF. As we know, the vibrational constants of high-lying excited states of NiF are generally similar and are around 650 cm^{-1}.[17] Assuming that the [19.7] $^2\Pi_{3/2}$ $v = 1$ level is not perturbed by any other level, it should lie near 20 370 cm^{-1}, and the separation between the [19.7] $^2\Pi_{3/2}$ $v = 1$ and the [20.3] $\Omega = {}^3/_2$ $v = 0$ level would be less than 100 cm^{-1}. As the two vibrational levels of the two excited states are very close, the large interaction between them causes the unusual isotopic shifts

and pushes the $v = 1$ level of [19.7] $^2\Pi_{3/2}$ higher in energy, resulting in an unusually large $\Delta G_{1/2}$ for the [19.7] $^2\Pi_{3/2}$ state. The same interaction occurs between the $v = 2$ level of [19.7] $^2\Pi_{3/2}$ and the $v = 1$ level of [20.3] $\Omega = {}^3/_2$ and between the $v' = 3$ level of [19.7] $^2\Pi_{3/2}$ and the $v = 2$ level of [20.3] $\Omega = {}^3/_2$, although the transition associated with $v' = 3$ level of [19.7] $^2\Pi_{3/2}$ has not been observed experimentally. We also noticed that the rotational constant of the $v = 1$ level of the [19.7] $^2\Pi_{3/2}$ state is irregular compared to the other excited states of NiF.[19] This may also be caused by the interaction between the [19.7] $^2\Pi_{3/2}$ state and the close-lying [20.3] $\Omega = {}^3/_2$ state, as the latter has an unusually large rotational constant.

4.4. Comparison between [19.7] $^2\Pi_{3/2}$ and [22.9] $^2\Pi_{3/2}$ States. It is interesting to compare the two $^2\Pi_{3/2}$ excited states, [19.7] $^2\Pi_{3/2}$ and [22.9] $^2\Pi_{3/2}$. Although they are located in different energy regions, their rotational constants are very similar. From the previous report,[17] the [19.7] $^2\Pi_{3/2}$ state correlates with the ^{2}D state of the Ni^+ ion, while the [22.9] $^2\Pi_{3/2}$ state correlates with $3d^8(^3P)4s^1$, ^{2}P state of Ni^+. Because these states derive from different ion states, their lifetimes are different, with the lifetime of the [19.7] $^2\Pi_{3/2}$ state being about 4 times longer than that of the [22.9] $^2\Pi_{3/2}$ state (see Table 4). In addition, transitions involving the $^2\Pi_{1/2}$ spin−orbit component of the [19.7] $^2\Pi_{3/2}$ state have not yet been observed, while the transition involving the [23.5] $^2\Pi_{1/2}$ spin−orbit component of the [22.9] $^2\Pi_{3/2}$ state appears with considerable intensity. Therefore, we may conclude that the former may follow Hund's case a coupling, while the latter displays a tendency toward Hund's case c coupling, where $\Delta\Sigma = 0$ is not a good selection rule, but $\Delta\Omega = 0, \pm 1$ is.

5. Conclusion

With the help of the isotopic shift measurements in this work and vibrational constants determined by B. Pinchemel's group, the vibrational assignments of numerous bands recorded in 17500−25000 cm^{-1} region were achieved unambiguously and, then, confirmed by identifying rotational profiles. Twelve bands involving different vibrational levels of the four upper states, [18.1] $^2\Delta_{5/2}$, [20.0] $^2\Delta_{5/2}$, [20.3] $\Omega = {}^3/_2$ and [22.9] $^2\Pi_i$, and the ground $X^2\Pi_{3/2}$ state have been rotationally analyzed. The molecular constants of these four high-lying excited states are determined for the first time. In addition, the lifetimes of the five excited states are measured under collision-free conditions. On the basis of the spectroscopic data and lifetime measurements, the electronic structure and interactions of these high-lying electronic states are discussed.

Acknowledgment. The authors are greatly indebted to the reviewer of this paper for his kind revisions and enlightening comments. This work was supported by the Chinese National Natural Science Foundation (Grant No. 20073040) and Chinese National Key Basic Research Special Foundation (Grant No. 1999075304).

Supporting Information Available: The line positions of the 12 transitions of NiF in the 17500−25000 cm^{-1} region. This material is available free of charge via the Internet at http://pubs.acs.org.

References and Notes

(1) Gray, J. A.; Li, M.; Nelis, T.; Field, R. W. *J. Chem. Phys.* **1991**, *95*, 7164.
(2) Merer, A. J. *Annu. Rev. Phys. Chem.* **1989**, *40*, 407.
(3) Hirao, T.; Dufour, C.; Pinchemel, B.; Bernath, P. F. *J. Mol. Spectrosc.* **2000**, *202*, 53.
(4) Poclet, A.; Krouti, Y.; Hirao, T.; Pinchemel, B.; Bernath, P. F. *J. Mol. Spectrosc.* **2000**, *204*, 125.
(5) Krishnamurty, V. G. *Indian J. Phys.* **1953**, *27*, 354.
(6) Gopal, R.; Joshi, M. M. *Curr. Sci.* **1981**, *50*, 530.
(7) Gopal, R.; Singh, L. K.; Joshi, M. M. *Indian J. Phys.* **1981**, *B55*, 507.
(8) Bai, J.; Hilborn, C. *Chem. Phys. Lett.* **1986**, *128*, 133.
(9) Pinchemel, B.; Lefebvre, Y.; Schamps, J. *J. Mol. Spectrosc.* **1979**, *77*, 29.
(10) Pinchemel, B. *J. Phys.* **1981**, *B14*, 2569.
(11) Dufour, C.; Carette, P.; Pinchemel, B. *J. Mol. Spectrosc.* **1991**, *148*, 303.
(12) Dufour, C.; Hikmet, I.; Pinchemel, B. *J. Mol. Spectrosc.* **1993**, *158*, 392.
(13) Dufour, C.; Hikmet, I.; Pinchemel, B. *J. Mol. Spectrosc.* **1994**, *165*, 398.
(14) Bouddou, A.; Dufour, C.; Pinchemel, B. *J. Mol. Spectrosc.* **1994**, *168*, 477.
(15) Dufour, C.; Pinchemel, B. *J. Mol. Spectrosc.* **1995**, *173*, 70.
(16) Focsa, C.; Dufour, C.; Pinchemel, B. *J. Mol. Spectrosc.* **1997**, *182*, 65.
(17) Carette, P.; Dufour, C.; Pinchemel, B. *J. Mol. Spectrosc.* **1993**, *161*, 323.
(18) Chen, Y.; Jin, J.; Hu, C. J.; Yang, X. L.; Ma, X. X.; Chen, C. X. *J. Mol. Spectrosc.* **2000**, *203*, 37.
(19) Jin, J.; Chen, Y.; Yang, X. L.; Ran, Q.; Chen, C. X. *J. Mol. Spectrosc.* **2001**, *208*, 18.
(20) Herzberg, G. *Spectra of Diatomic Molecules*; Van Nostrand: Princeton, NJ, 1950.
(21) Bernath, P. F. *Spectra of Atoms and Molecules*; New York, Oxford, 1995.
(22) Brown, J. M.; Cheung, A. S.-C.; Merer, A. J. *J. Mol. Spectrosc.* **1987**, *124*, 464.
(23) Lefebvre-Brion, H.; Field, R. W. *Perturbations in the Spectra of Diatomic Molecules*, 1st ed.; Academic Press: Orlando, FL, 1986.